SUPPLEMENTARY MATERIAL

MATERIALS AND METHODS

MDM2 PROTAC YX-02-030 synthesis and NMR spectra

All commercially obtained solvents and reagents were used as received. Flash column chromatography was performed using silica gel 60 (230-400 mesh). Analytical thin layer chromatography (TLC) was carried out on Merck silica gel plates with QF-254 indicator and visualized by UV, PMA, or KMnO4. ^{1}H and ^{13}C NMR spectra were recorded on a Bruker Advance 400. Chemical shifts are reported in parts per million (ppm, δ) using the residual solvent line as a reference. Splitting patterns are designated using the following abbreviations: s, singlet; d, doublet; t, triplet; dd, doublet of doublet; m, multiplet; br, broad. Coupling constants (J) are reported in hertz (Hz). Tetramethylsilane was used as an internal standard for proton nuclear magnetic resonance for samples run in $CDCl_3$ or DMSO-d_6. LC−MS data were acquired on a Waters Acquity UPLC/MS system equipped with a UPLC binary pump, an SQD 3100 mass spectrometer with an electrospray ionization (ESI) source and a PDA detector (210−400 nm). High-resolution mass spectra were obtained using the Q Exactive HF-X mass spectrometer which provided high-resolution, accurate mass, and total ion and extracted ion chromatograms. All compounds tested were present within a 5 ppm mass error. The purity of all final compounds was determined by HPLC, and the compounds are at least ≥95% pure.

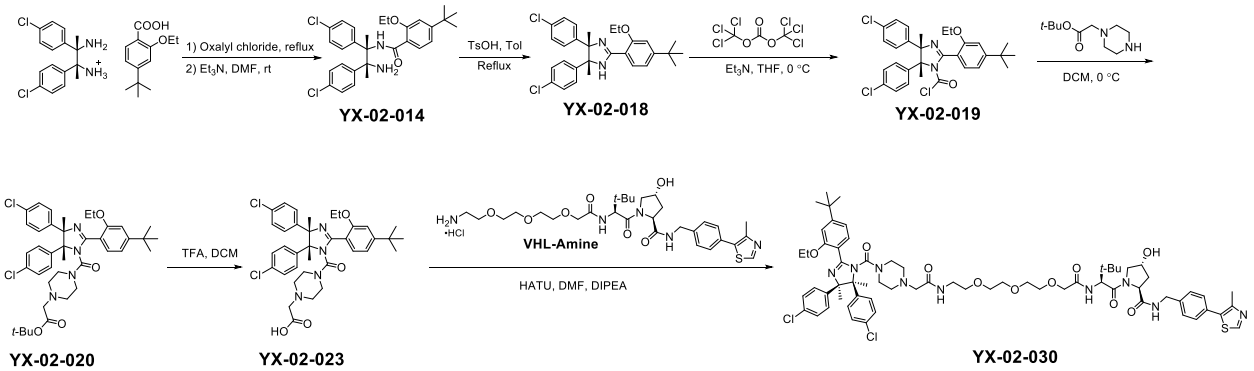

***N*-((2*S*,3*R*)-3-amino-2,3-bis(4-chlorophenyl)butan-2-yl)-4-tert-butyl-2-ethoxybenzamide (YX-02-014)**

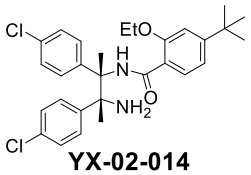

YX-02-014
Batch # JG-02-047

4-(*tert*-butyl)-2-ethoxy-benzoyl acid (666 mg, 3.0 mmol) was dissolved in toluene and treated with oxalyl chloride (320 µL) then stirred at 50 ºC for 1h and then the reaction solvent was removed by roto-evaporation, and the residue was used directly for the next step. A mixture of the obtained product and triethylamine (823 µL, 6.0 mmol) in DCM (15 mL) was reacted with 2,3-bis-(4-chlorophenyl)-2, 3-butanediamine (840 mg, 3.0 mmol) for 30 min at room temperature. The mixture was partitioned between 10% sodium bicarbonate solution and dichloromethane. The organic phase was separated and washed with water, dried over anhydrous sodium sulfate, concentrated, and purified by chromatography on silica gel to afford YX-02-014 (JG-02-047) (600 mg, 43% yield). LCMS: m/z calculated for $C_{29}H_{34}Cl_2N_2O_2$ = 512.20; found $[M+H]^+$ = 513.14.

(4*S*,5*R*)-2-(4-tert-butyl-2-ethoxyphenyl)-4,5-bis(4-chlorophenyl)-4,5-dimethyl-4,5-dihydro-1*H*-imidazole (YX-02-018)

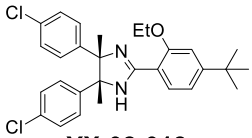

YX-02-018
Batch # JG-02-050

YX-02-014 (300 mg, 0.58 mmol) was dissolved in Toluene (15 mL) and treated with TsOH (20 mg, 0.116 mmol) and heated to reflux for 4h, then the solvent was removed, and the residue was purified by chromatography on silica gel to afford YX-02-018 (JG-02-050) (220 mg, 73% yield) ^{1}H NMR (400 MHz, $CDCl_3$) δ 10.72 (brs, 1H), 9.08 (d, *J* = 8.4 Hz, 1H), 7.39 (dd, *J* = 8.4, 1.4 Hz,

1H), 7.09 – 7.06 (m, 1H), 7.03 (d, *J* = 8.6 Hz, 4H), 6.83 (d, *J* = 8.7 Hz, 4H), 4.33 (q, *J* = 6.9 Hz, 2H), 1.98 (s, 6H), 1.47 (t, *J* = 6.9 Hz, 3H), 1.38 – 1.33 (3, 9H). LCMS: m/z calculated for $C_{29}H_{32}Cl_2N_2O_2$ = 494.19; found $[M+H]^+$ = 495.04.

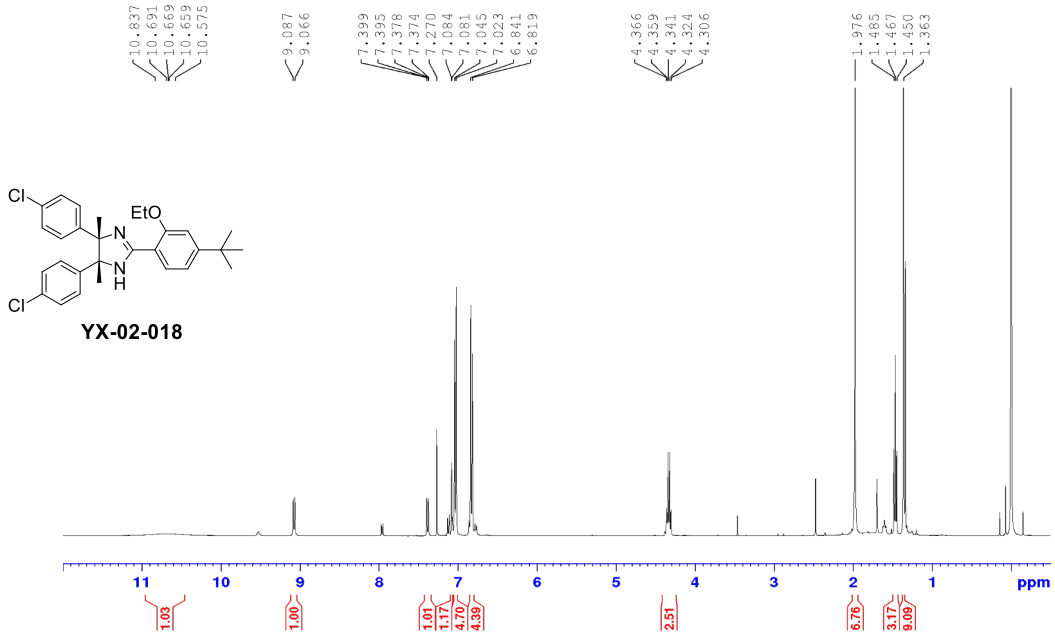

^{1}H NMR (400 MHz, $CDCl_3$) spectrum of compound of YX-02-018.

(4*S*,5*R*)-2-(4-tert-butyl-2-ethoxyphenyl)-4,5-bis(4-chlorophenyl)-4,5-dimethyl-4,5-dihydro-1*H*-imidazole-1-carbonyl chloride (YX-02-019)

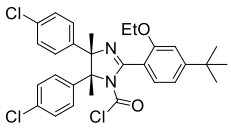

YX-02-019
Batch # JG-02-060

To a solution of YX-02-018 (220 mg, 0.44 mmol) and triethylamine (300µL, 2.2 mmol) in DCM (15 mL) at 0 ºC was added triphosgene (600 mg, 2.0 mmol). After stirring for 30 min the mixture was taken up and washed with water, dried over anhydrous sodium sulfate, concentrated to afford YX-02-019 (JG-02-060) (200 mg) and the residue was used directly for next step.

Tert-butyl-2-(4-((4*S*,5*R*)-2-(4-tert-butyl-2-ethoxyphenyl)-4,5-bis(4-chlorophenyl)-4,5-dimethyl-4,5-dihydro-1*H*-imidazole-1-carbonyl)piperazin-1-yl)acetate (YX-02-020)

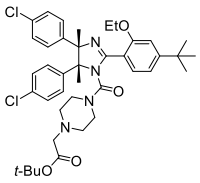

YX-02-020
Batch # JG-02-062

To a solution of YX-02-019 (120 mg, 0.214 mmol) and *tert*-butyl 2-(piperazin-1-yl) acetate (80 mg, 0.428 mmol) in DCM (10 mL) at 0 ºC was added triethylamine (240 µL, 2 mmol). The reaction was allowed to react for 24h. The mixture was partitioned between 10% sodium bicarbonate solution and dichloromethane. The organic phase was separated and washed with water, dried over anhydrous sodium sulfate, concentrated, and purified by chromatography on silica gel to afford YX-02-020 (JG-02-062) (150 mg, 99% yield). ^{1}H NMR (400 MHz, $CDCl_3$) δ 7.60 (d, J = 8.0 Hz, 1H), 7.00 (dd, J = 8.0, 1.3 Hz, 1H), 7.02 – 6.88 (m, 9H), 4.20 – 4.05 (m, 1H), 4.00 – 3.88 (m, 1H), 3.29 – 3.19 (m, 1H), 3.20 – 3.10 (m, 1H), 3.08 – 2.97 (m, 1H), 2.86 – 2.80 (m, 1H), 2.78 (s, 2H), 2.34 (brs, 1H), 2.25 – 2.14 (m, 1H), 1.92 (s, 3H), 1.86 – 1.76 (m, 1H), 1.60 (s, 3H), 1.55 (brs, 1H), 1.39 (d, J = 2.3 Hz, 1H), 1.38– 1.33 (m, 11H), 1.30 (s, 9H). LCMS: m/z calculated for $C_{40}H_{50}Cl_2N_4O_4$ = 720.32; found $[M+H]^+$ = 721.35.

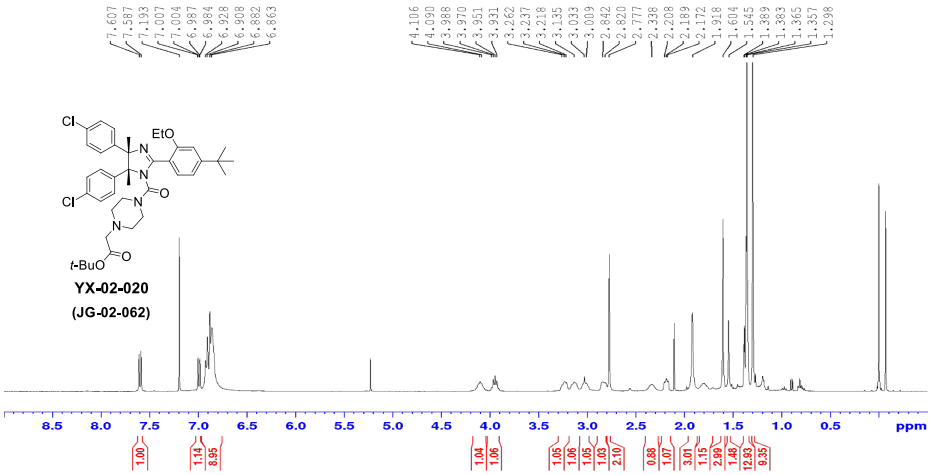

^{1}H NMR (400 MHz, $CDCl_3$) spectrum of compound of YX-02-020 (JG-02-062)

2-(4-((4*S*,5*R*)-2-(4-tert-butyl-2-ethoxyphenyl)-4,5-bis(4-chlorophenyl)-4,5-dimethyl-4,5-dihydro-1*H*-imidazole-1-carbonyl)piperazin-1-yl)acetic acid (YX-02-023)

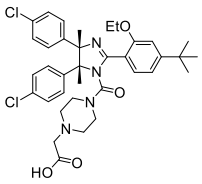

YX-02-023
Batch # JG-02-067

YX-02-20 (150 mg, 0.2 mmol) was dissolved in DCM (5 mL) and treated with TFA (1 mL), after stirred for 18 h, remove the reaction solvent, then redissolved in MeOH and DCM and concentrated, and purified by chromatography on silica gel to afford YX-02-023 (JG-02-067) (120 mg, 86% yield). ^{1}H NMR (400 MHz, MeOD) δ 7.70 (d, *J* = 8.0 Hz, 1H), 7.21 (dd, *J* = 8.0, 1.5 Hz, 1H), 7.17 (d, *J* = 1.4 Hz, 1H), 7.11 – 6.88 (m, 8H), 4.30 – 4.20 (m, 1H), 4.17 – 4.06 (m, 1H), 3.30 – 3.25 (m, 3H), 3.24 – 3.17 (m, 1H), 3.14 – 3.09 (m, 1H), 3.07 (s, 2H), 2.94 – 2.81 (m, 1H), 2.80 – 2.67 (m, 1H), 2.01 (s, 3H), 1.74 (s, 3H), 1.46 – 1.40 (m, 12H).^{13}C NMR (100 MHz, MeOD) δ 159.21, 157.46, 157.32, 154.95, 140.75, 139.94, 132.41, 132.02, 131.37, 128.17, 127.15, 126.82, 117.63, 116.13, 108.39, 76.43,76.16, 63.97, 59.35, 51.68, 34.96, 30.34, 23.86, 22.59, 19.43, 13.68. LCMS: m/z calculated for $C_{36}H_{42}Cl_2N_4O_4$ = 664.26; found $[M+H]^+$ = 665.27; HRMS (ESI): calculated for $C_{36}H_{43}Cl_2N_4O_4$ $[M + H]^+$ 665.26614, found 665.26245.

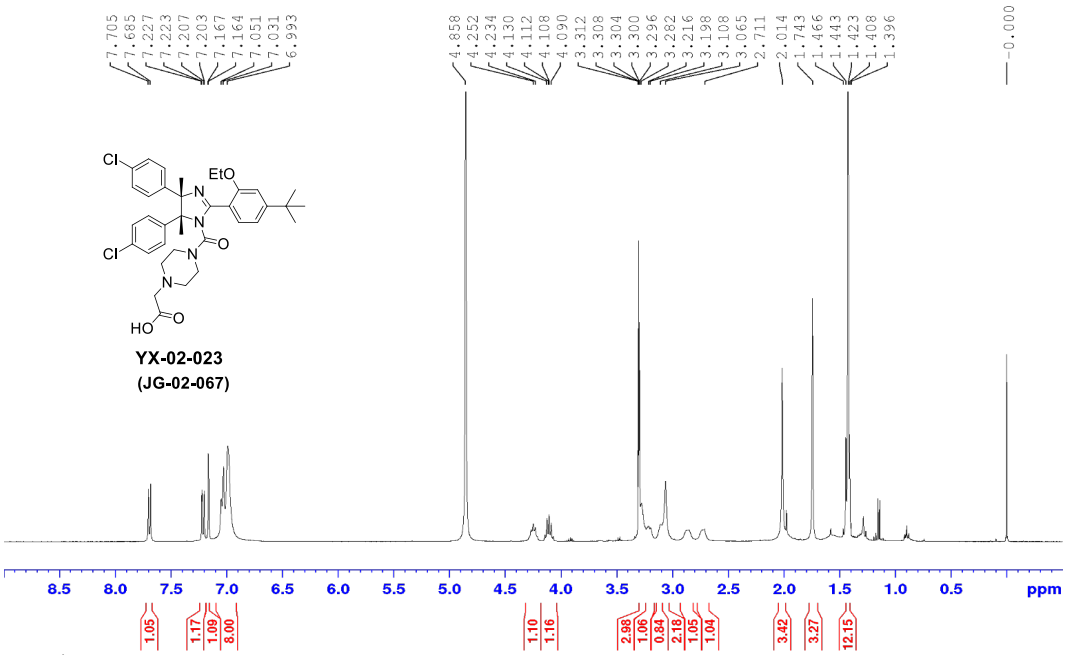

^{1}H NMR (400 MHz, MeOD) spectrum of compound of YX-02-023 (JG-02-067)

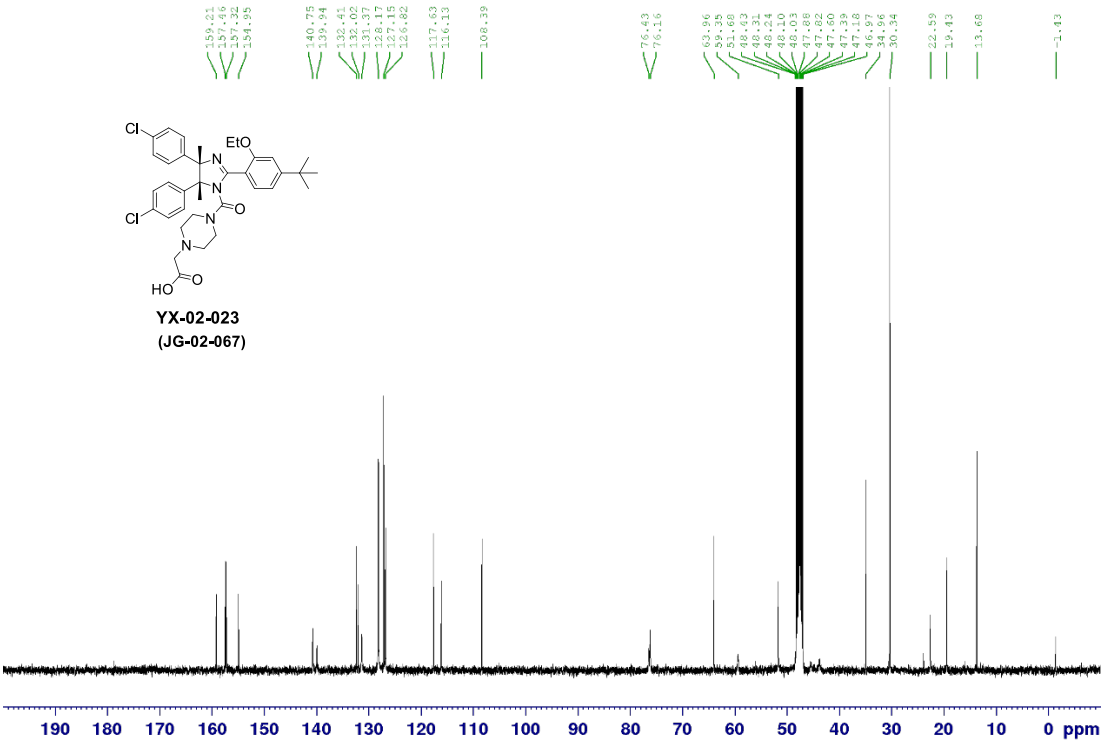

^{13}C NMR (100 MHz, MeOD) spectrum of compound of YX-02-023 (JG-02-067)

(2*S*,4*R*)-1-((*S*)-2-tert-butyl-17-(4-((4*R*,5*S*)-2-(4-tert-butyl-2-ethoxyphenyl)-4,5-bis(4-chlorophenyl)-4,5-dimethyl-4,5-dihydro-1*H*-imidazole-1-carbonyl)piperazin-1-yl)-4,16-dioxo-6,9,12-trioxa-3,15-diazaheptadecane)-4-hydroxy-*N*-(4-(4-methylthiazol-5-yl)benzyl)pyrrolidine-2-carboxamide (YX-02-030)

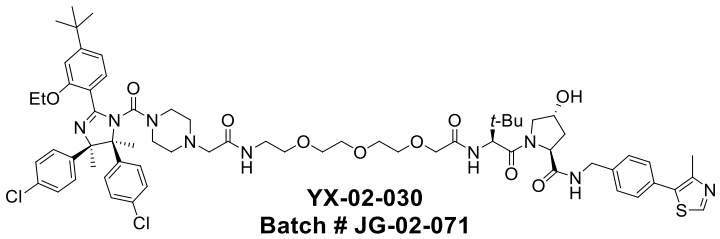

A mixture of VHL-Amine (1) (31 mg, 0.05 mmol) and YX-02-023 (JG-02-067) (36 mg, 0.05 mmol) in DMF (3 mL) was treated with DIPEA (16 µL, 0.1 mmol) and then HATU (20 mg, 0.05 mmol) and stirred at ambient temperature for 1 hour. After which time the reaction mixture was diluted with H_2O and extracted with EtOAc. The organic layer was washed with saturated sodium bicarbonate solution and dried over Na_2SO_4. Removal of the solvent gave a crude product that was purified by chromatography on silica to afford YX-02-030 (JG-02-071) (28 mg, 50% yield). ^{1}H NMR (400 MHz, DMSO-d_6) δ 8.99 (s, 1H), 8.59 (t, J = 6.0 Hz, 1H), 7.62 – 7.52 (m, 2H), 7.45 – 7.37 (m, 5H), 7.11 – 6.95 (m,9H), 5.15 (d, J = 2.7 Hz, 1H), 4.57 (d, J = 9.6 Hz, 1H), 4.48 – 4.40 (m, 1H), 4.41 – 4.33 (m, 2H), 4.31 – 4.19 (m, 2H), 4.01 – 3.91 (m, 3H), 3.68 (dd, J = 10.6, 3.8 Hz, 1H), 3.64 – 3.59 (m, 3H), 3.58 – 3.54 (m, 2H), 3.54 – 3.51 (m, 2H), 3.50 – 3.47 (m, 2H), 3.40 – 3.34 (m, 2H), 3.24 – 3.12 (m, 3H), 3.02 – 2.85 (m, 3H), 2.61 (brs, 2H), 2.45 (s, 4H), 2.30 – 2.18 (m, 1H), 2.10 – 2.02 (m, 1H), 1.95 – 1.90 (m, 4H), 1.89 (s, 3H), 1.60 (s, 3H), 1.52 – 1.44 (m, 1H), 1.36 (s, 9H), 1.29 (t, J = 6.9 Hz, 10H), 0.95 (s, 9H). ^{13}C NMR (100 MHz, DMSO-d_6) δ 172.21, 171.79, 169.94, 169.58, 169.20, 169.03, 157.71, 157.34, 156.23, 155.37, 151.92, 148.21, 142.34, 141.62, 139.90, 131.94, 131.60, 131.28, 130.86, 130.17, 129.35, 129.15, 129.02, 128.61, 127.93, 127.43, 126.88, 117.48, 108.85, 76.67, 75.45, 70.90, 70.30, 70.09, 69.34, 64.05, 61.48, 59.20,

57.03, 56.15, 52.06, 51.83, 42.15, 38.49, 38.39, 36.19, 35.42, 31.55, 26.74, 26.65, 24.36, 20.68, 16.39, 14.67. LCMS: m/z calculated for $C_{66}H_{85}Cl_2N_9O_{10}S$ = 1265.55; found LC-MS $[(M+2H)/2]^+$ = 634.99, RT =2.67 min; HRMS (ESI): calculated for $C_{66}H_{85}Cl_2N_9O_{10}S$ $[M+H]^+$ 1266.55954, found 1266.55396.

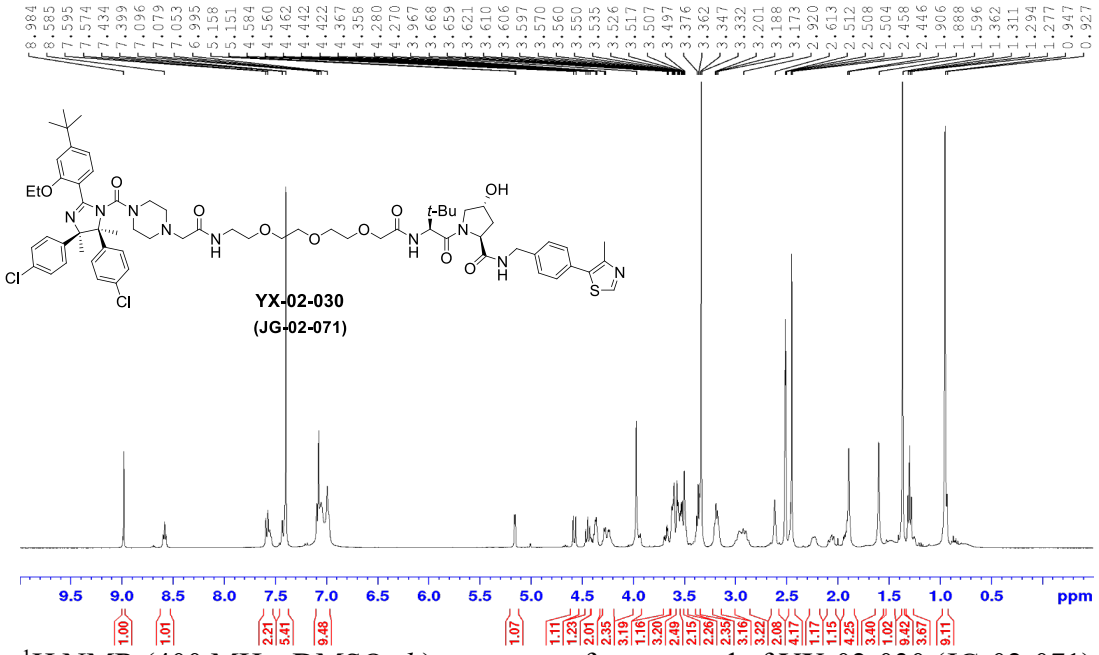

^{1}H NMR (400 MHz, DMSO-d_6) spectrum of compound of YX-02-030 (JG-02-071)

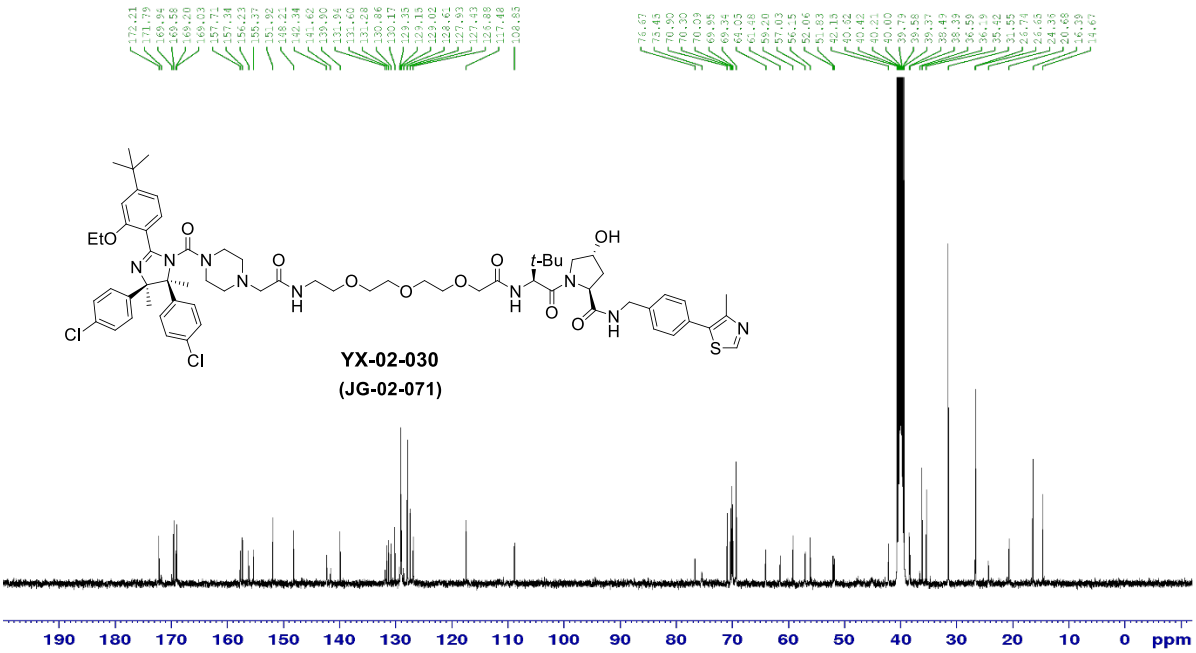

^{13}C NMR (100 MHz, DMSO-d_6) spectrum of compound of YX-02-030 (JG-02-071)

HTRF binding assays

Inhibition of MDM2 binding to p53 using HTRF technology

Both GST-MDM2 and HIS-p53 were expressed *E. coli* and purified by affinity chromatography. pGEX-4T MDM2 WT was provided by Dr. Mien-Chie Hung (RRID:Addgene _RRID: 16237) and human p53-(1-393) was a provided by Dr. Cheryl Arrowsmith (RRID:Addgene_24859). HTRF assays contained 1 nM GST-MDM2, 0.7 nM HIS-p53, 0.3 nM of anti-GST-Tb HTRF donor (RRID:AB_2927626) and 4 nM of anti-HIS-d2 HTRF acceptor (RRID:AB_2884027) antibodies (PerkinElmer CisBio) in 10 uL of 10 mM HEPES, pH 7.4, 100 mM NaCl, 5 mM MgCl2, 5 mM DTT, 0.01% Triton X-100 in white low-volume 384-well plates. Both GST-MDM2 and HIS-p53 were pre-incubated with their respective HTRF antibodies for 15 min. Test compounds were solubilized at 10 mM in DMSO and concentration series was added to the assay plate using the Echo 650 acoustic liquid handling system by direct dilution. The final amount of DMSO added to the assay was 100 nL (0.1%). Compounds were pre-incubated with 5uL of GST-MDM2 for 15-30 min before 5 uL of HIS-p53/anti-HIS-d2 was added to the assay. After a 2 hr incubation, the HTRF signal was measured using the ClarioStar plate reader (BMG Labtech). Data were then normalized to % inhibition, where 0% is the HTRF signal in the absence of compound, and 100% is the HTRF signal in the absence of GST-MDM2. IC_{50} values were determined from nonlinear regression fits of a data to a four parameter dose-response equation using XLFit (IDBS, RRID:SCR_004077). Data are the means ± SEM of three replications.

Inhibition of HIF-1α peptide binding to the VHL complex using HTRF technology

Assays contained 2 nM of HIS-VHL complex (R&D systems, E3-655-025), 2 nM of biotin-hydroxyproline-HIF1α peptide (Biotin-DLDLEMLAXYIPMDDDFQL, X=hydroxyproline), 0.3 nM anti-HIS-Tb HTRF donor (RRID:AB_2716834) antibody and 4 nM streptavidin-d2 HTRF

acceptor (RRID:SCR_023093) (PerkinElmer CisBio) in a final volume of 10 uL of 25 mM HEPES, pH 7.4, 150 mM NaCl, 5 mM DTT, 0.005% Tween20 in white low volume 384-well plates. Both HIS-VHL complex and biotin-HIF1α peptide were pre-incubated with their respective HTRF antibodies for 15 min. Test compounds were solubilized at 10 mM in DMSO and concentration series was added to the assay plate using the Echo 650 acoustic liquid handling system by direct dilution. The final amount of DMSO added to the assay was 100 nL (0.1%). Compounds were pre-incubated with HIS-VHL complex before the addition of the biotin-HIF1α peptide. After a 2 hr incubation, the HTRF signal was measured using the ClarioStar plate reader (BMG Labtech). Data were then normalized to % inhibition, where 0% is the HTRF signal in the absence of compound, and 100% is the HTRF signal in the absence of HIS-VHL. IC_{50} values were determined from nonlinear regression fits of a data to a four parameter dose-response equation using XLFit (IDBS, RRID:SCR_004077). Data are the means ± SEM of three replications.

SPR binding kinetics and affinity analysis

Association and dissociation rate constants for compounds were determined using a Biacore T200 SPR instrument. Approximately 4000 RU of HIS-SUMO-MDM2 (expressed and purified) was immobilized on a multidentate linear carboxylate high affinity nickel chip (NIHC1500M, Xantec Bioanalytics). The running buffer was 10mM HEPES pH 7.4, 150mM NaCl, 5mM $MgCl_2$, 0.5mM TCEP, 0.005% Tween-20, 2% DMSO. Test compounds were serially diluted in 100% DMSO at 50X final concentration and then diluted into running buffer without DMSO such that the DMSO concentration of the sample and the running buffer was approximately the same. Solvent correction cycles were also included to control for bulk effects due to small DMSO differences. The association time was 60s and the dissociation time was 360s at a flow rate of 30uL/min. After each sample injection, the needle was washed with 50% DMSO to limit compound carry over. Kinetic

data were globally fit to a single site binding model using Biacore evaluation software (RRID:SCR_008424).

AlphaScreen for ternary complex formation

GST-MDM2 (8 nM) was pre-incubated with glutathione AlphaScreen donor beads and HIS-VHL complex (8 nM, RD systems: E3-655-025) was pre-incubated with nickel chelate AlphaScreen acceptor beads for 30 min at room temperature in 10 mM HEPES, pH 7.4, 100 mM NaCl, 5 mM MgCl2, 0.01% TX100, 5 mM DTT. Dose-response curves of test compounds in 100% DMSO were added to a low volume, white, 384-well microplate using the Echo 650 acoustic liquid handler by direct dilution such the final concentration of DMSO in the assay was 1%. Assays were initiated by adding 5 uL of GST-MDM2/AlphaScreen donor bead mix and 5 uL of HIS-VHL complex/AlphaScreen acceptor bead mix to give a final volume of 10 uL. After 90 min pre-incubation at room temperature, the AlphaScreen signal was measured using the ClarioStar plate reader. Data were fit to a bell-shaped dose-response curve equation in GraphPad Prism (RRID:SCR_002798).

RNA-sequencing analysis

Fastq files of RNA-seq data were analyzed with FASTQC (RRID:SCR_014583, version 0.11.8) to check sequencing read quality. To determine strand specificity, infer_experiment.py script from RSeQC (RRID:SCR_005275), was used (2). To trim the adapter sequences, Cutadapt (RRID:SCR_011841, version 2.4) was employed (3). We mapped the reads to the human reference genome (Ensembl version GRCh38, RRID:SCR_002344) and assembled transcripts using Hisat2 (RRID:SCR_015530, version 2.1.0) and StringTie (RRID:SCR_016323, version 1.3.6), respectively (4,5). A python script, prepDE, was used to extract read count information. Read

counts were imported into edgeR (RRID:SCR_012802) (6) to normalize the data and then compute differential gene expression in PROTAC-treated or *MDM2* knockdown cells compared to DMSO vehicle control or non-targeting shRNA control, respectively. Results were adjusted using the Benjamini-Hochberg (BH) multiple testing correction methods (7).

In vivo mouse and human CD34+ toxicity testing

For toxicity testing of C57Bl/6 mice (Jackson Labs; RRID:MGI:2159769), twice daily intraperitoneal (IP) injections of MDM2-PROTAC at 50mg/kg in 10% DMSO, 10% solutol, and 80% PBS or vehicle control were administered for 8 days. Following the last dose, blood and tissues from the mice were collected, processed, and analyzed, as described in the Materials and Methods in the manuscript. Blood and tissues were also collected from the nude mice in the xenograft experiments 13 days after treatment began or at the time of euthanasia, respectively (see Materials and Methods in the manuscript).

To evaluate p53 pathway activation in normal mouse hematopoietic cells, C57Bl/6 mice (Jackson Labs; RRID:MGI:2159769) received 3 consecutive daily IP injections of 50mg/kg of MDM2-PROTAC or vehicle control (n=3/group, equal distribution of males and females). Following 72hr of treatment, splenocytes (following red blood cell lysis with Gey's solution) and whole bone marrow and were isolated for protein (Western blotting) and mRNA (qRT-PCR) evaluation (see Materials and Methods in the manuscript; primer sequences were previously published (8)). As a positive control for p53 activation, two mice were euthanized 4hr after being gamma irradiated (10Gy).

De-identified human CD34+ hematopoietic cells leftover from bone marrow transplantation were treated with MDM2-PROTAC, RG7112D, RG7112, or DMSO vehicle control. Viability of the CD34+ cells was determined using a fluorescent live-dead flow cytometric

assay (Abcam #ab115347) and expression of p53 target genes was measured by qRT-PCR (see Materials and Methods in manuscript and primer sequences in Supplementary Table S3).

REFERENCES (for SUPPLEMENTARY MATERIALS AND METHODS above)

1. Ottis P, Toure M, Cromm PM, Ko E, Gustafson JL, Crews CM. Assessing Different E3 Ligases for Small Molecule Induced Protein Ubiquitination and Degradation. ACS Chem Biol **2017**;12(10):2570-8 doi 10.1021/acschembio.7b00485.

2. Wang L, Wang S, Li W. RSeQC: quality control of RNA-seq experiments. Bioinformatics **2012**;28(16):2184-5 doi 10.1093/bioinformatics/bts356.

3. Martin M. Cutadapt removes adapter sequences from high-throughput sequencing reads. EMBNetjournal **2011**;17:10-2.

4. Kim D, Paggi JM, Park C, Bennett C, Salzberg SL. Graph-based genome alignment and genotyping with HISAT2 and HISAT-genotype. Nat Biotechnol **2019**;37(8):907-15 doi 10.1038/s41587-019-0201-4.

5. Pertea M, Kim D, Pertea GM, Leek JT, Salzberg SL. Transcript-level expression analysis of RNA-seq experiments with HISAT, StringTie and Ballgown. Nat Protoc **2016**;11(9):1650-67 doi 10.1038/nprot.2016.095.

6. Robinson MD, McCarthy DJ, Smyth GK. edgeR: a Bioconductor package for differential expression analysis of digital gene expression data. Bioinformatics **2010**;26(1):139-40 doi 10.1093/bioinformatics/btp616.

7. Benjamini Y, Hochberg Y. Controlling the False Discovery Rate - a Practical and Powerful Approach to Multiple Testing. J Roy Stat Soc B Met **1995**;57(1):289-300.

8. Feeley KP, Adams CM, Mitra R, Eischen CM. Mdm2 Is Required for Survival and Growth of p53-Deficient Cancer Cells. Cancer Res **2017**;77(14):3823-33 doi 10.1158/0008-5472.CAN-17-0809.

TABLES

Supplementary Table S1. TNBC patient characteristics.

Sample ID	Gender	Age	Race	Ethnicity	Relapse
TNBC-1	Female	57	Black/African American	Not Hispanic/Latino	UN
TNBC-2	Female	42	Black/African American	Not Hispanic/Latino	UN
TNBC-3	Female	78	Black/African American	Not Hispanic/Latino	Yes
TNBC-4	Female	64	White	Not Hispanic/Latino	Yes
TNBC-5	Female	49	Black/African American	Not Hispanic/Latino	UN

UN-Unknown

Supplementary Table S2. Antibodies used in current study.

Antibody specificity and/or clone	Source	Cat. #	RRID	Purpose*
MDM2 (2A10)	Millipore	#OP115	564806	WB and IP
MDM2 (3G9)	Millipore	#04-1530	10563796	WB (Fig S1C)
MDM2 (SMP14)	Santa Cruz	sc-965	627920	WB (Fig S1C)
MDM2 (D1V2Z)	Cell Signaling	#86934	2784534	WB (Fig S1C)
VHL	Cell Signaling	#68547	2716279	WB
Cleaved PARP (Asp214)	Cell Signaling	#9541	331426	WB
Cleaved Caspase 3 (Asp175)	Cell Signaling	#9661	2341188	WB and IHC
p53 (Ab7)	Millipore	#JA1308	213630	WB
TAp73 (5B429)	Novus	NBP2-24737	2927606	WB, IP, and ChIP
phospho-TAp73 (Tyr99)	Cell Signaling	#4665	2315158	WB
Acetylated lysine	Cell Signaling	#9441	331805	IP
ΔNp73 (38C674.2)	Novus	NBP2-24873	2927607	WB
TAp63	Abcam	ab53039	881860	WB
c-Abl	Cell Signaling	#2862	2257757	WB
phospho-c-Abl (Tyr412, 247C7)	Cell Signaling	#2865	331381	WB
CBP (D6C5)	Cell Signaling	#7389	2616020	WB and IP
p300 (RW128)	Millipore	#05-257	309670	WB and IP
BAX (N-20)	Santa Cruz	sc-493	2227995	WB
NOXA	Sigma	#PRS-2437	1854576	WB
PUMA	Abcam	ab9643	296537	WB
β-ACTIN (AC-74)	Sigma	#A5316	476743	WB
Mouse IgG control	Santa Cruz	sc-2025	737182	IP and ChIP
anti-GST-Tb donor	CisBio	61GSTTLF	2927626	HTRF
anti-HIS-d2 acceptor	CisBio	61GSTDL	2716833	HTRF
anti-HIS-Tb-Gold donor	CisBio	61HI2TL	2716834	HTRF
Streptavidin-d2 acceptor	CisBio	610SADLF	2928111	HTRF

*WB-Western blot; IP-Immunoprecipitation; IHC-Immunohistochemistry; ChIP-Chromatin immunoprecipitation; HTRF-Homogenous Time Resolved Fluorescence

Supplementary Table S3. Human primers used in current study.

Gene	Forward (5' → 3')	Reverse (5' → 3')	Purpose
BAX	CCCGAGAGGTCTTTTTCCGAG	CCAGCCCATGATGGTTCTGAT	qRT-PCR
NOXA	CGGGCTCTGTAGCTGAGTG	TTCTGCCGGAAGTTCAGTTT	qRT-PCR
PUMA	GACCTCAACGCACAGTACGAG	AGGAGTCCCATGATGAGATTGT	qRT-PCR
AEN	CTGGAGTGGCATCACTCGG	GGTGGACATACTTGAGCGCC	qRT-PCR
APAF1	GTCACCATACATGGAATGGCA	CTGATCCAACCGTGTGCAAA	qRT-PCR
TP53I3	GGAGGACCGGAAAACCTCTAC	CCTCAAGTCCCAAAATGTTGCT	qRT-PCR
PIDD1	GGAGGTATACGTGACCACCA	CACGGTAGAAGGACACCTGG	qRT-PCR
AchR	AGGACCCTACAGACCCCTCTTC	AGTGTTCATGGTGGCTAGGTG	qRT-PCR
MDM2	GTGAATCTACAGGGACGCCAT	CTGATCCAACCAATCACCTGAA	qRT-PCR
p73	GGATTCCAGCATGGACGTCTT	GCGCGGCTGCTCATCT	qRT-PCR
β-ACTIN	CACCAACTGGGACGACAT	ACAGCCTGGATAGCAACG	qRT-PCR
BAX	TAATCCCAGCGCTTTGGAA	TGCAGAGACCTGGATCTAGCAA	ChIP
NOXA	CAGCGTTTGCAGATGGTCAA	CCCCGAAATTACTTCCTTACAAAA	ChIP
PUMA	GCGAGACTGTGGCCTTGTGT	CGTTCCAGGGTCCACAAAGT	ChIP
AEN	CTGCTCTCGCCCGCCTCCCCGCTG	CTGAAGCCCCGCGTGTCTCTTCCGGTCTGCACG	ChIP
APAF1	CAGCCTCGCGTCCACTTACCAGG	CGGAAGAAGTCGGGGCCCAAGG	ChIP
TP53I3	CACTCCCAACGGCTCCTTT	GCCCATCTTGAGCATGGGT	ChIP
PIDD1	CTGCCTGGACAGGCCTGC	GCAGCTGCCTCCAGCTCTG	ChIP
AchR	CCTTCATTGGGATCACCACG	GGAGATGAGTACCAGCAGGTTG	ChIP
p53-seq-1	ATGGAGGAGCCGCAGTCAG	TGGGTGCTTCTGACGCACAC	Sequencing
p53-seq-2	AGGTTGGCTCTGACTGTACC		Sequencing

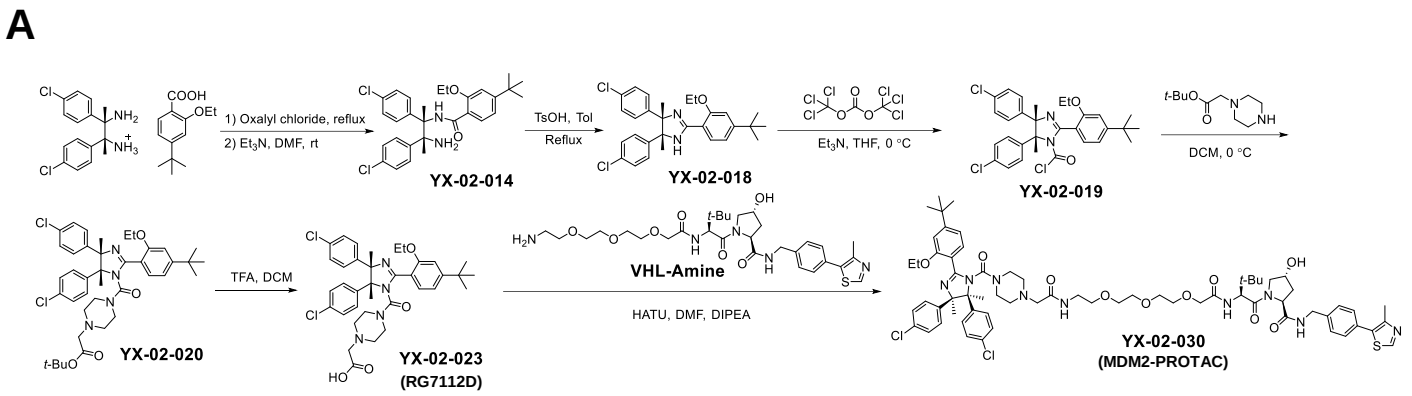
A
1) Oxalyl chloride, reflux
2) Et3N, DMF, rt
YX-02-014
TsOH, Tol
Reflux
YX-02-018
Et3N, THF, 0 °C
YX-02-019
DCM, 0 °C
TFA, DCM
YX-02-020
YX-02-023
(RG7112D)
VHL-Amine
HATU, DMF, DIPEA
YX-02-030
(MDM2-PROTAC)

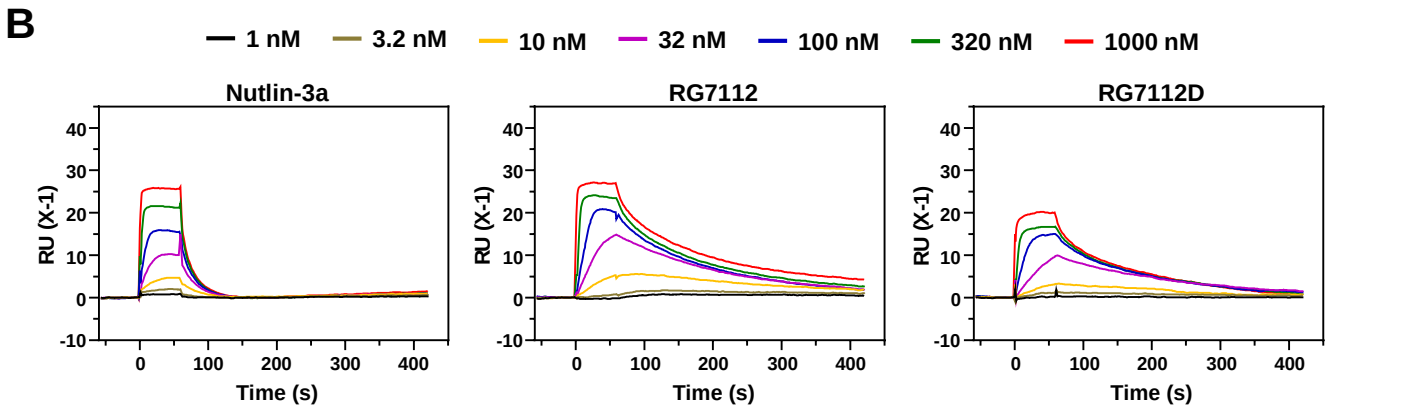
B
1 nM
3.2 nM
10 nM
32 nM
100 nM
320 nM
1000 nM
Nutlin-3a
RG7112
RG7112D
RU (X-1)
Time (s)

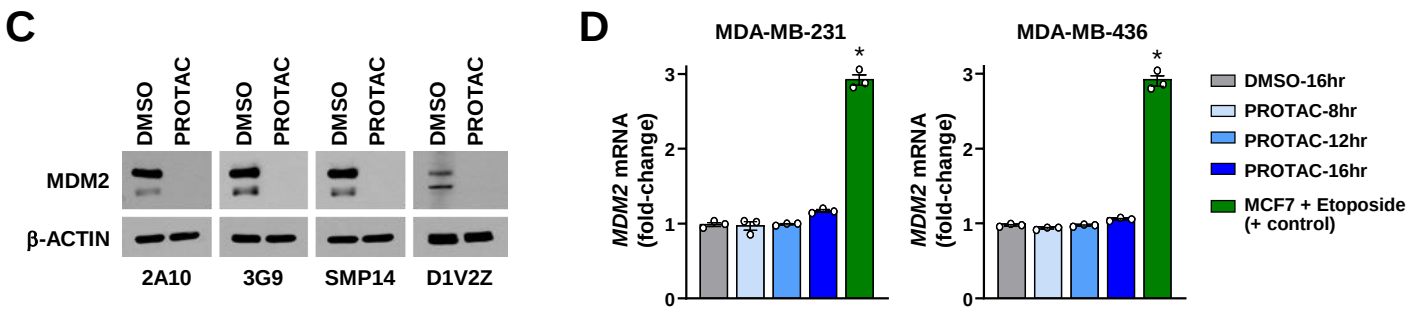
C
DMSO
PROTAC
MDM2
β-ACTIN
2A10
3G9
SMP14
D1V2Z
D
MDA-MB-231
MDA-MB-436
MDM2 mRNA
(fold-change)
DMSO-16hr
PROTAC-8hr
PROTAC-12hr
PROTAC-16hr
MCF7 + Etoposide
(+ control)

Supplementary Figure S1. Synthesis and binding analysis of the MDM2-PROTAC and detection of MDM2.

A, Chemical synthesis of the MDM2-PROTAC YX-02-030. **B**, Surface plasmon resonance (SPR) kinetic plots for the compounds indicated. Graphical data is a representative of a single experiment which was repeated three times with similar results. **C**, Western blots for MDM2 using multiple antibodies in MDA-MB-231 cells treated with MDM2-PROTAC (6μM, 16hr). **D**, qRT-PCR (quadruplicate) for *MDM2* expression in MDA-MB-231 and MDA-MB-436 cells treated with MDM2-PROTAC (6μM) or DMSO vehicle control for the indicated times; mean ± SEM. MCF7 breast cancer cells treated with etoposide (10μM, 24hr) served as a positive control for *MDM2* expression. Data from each cell line was made relative to its own DMSO control. For **D**, **P*<0.0001 (1-way ANOVA), comparing MDM2-PROTAC or etoposide to DMSO vehicle control.

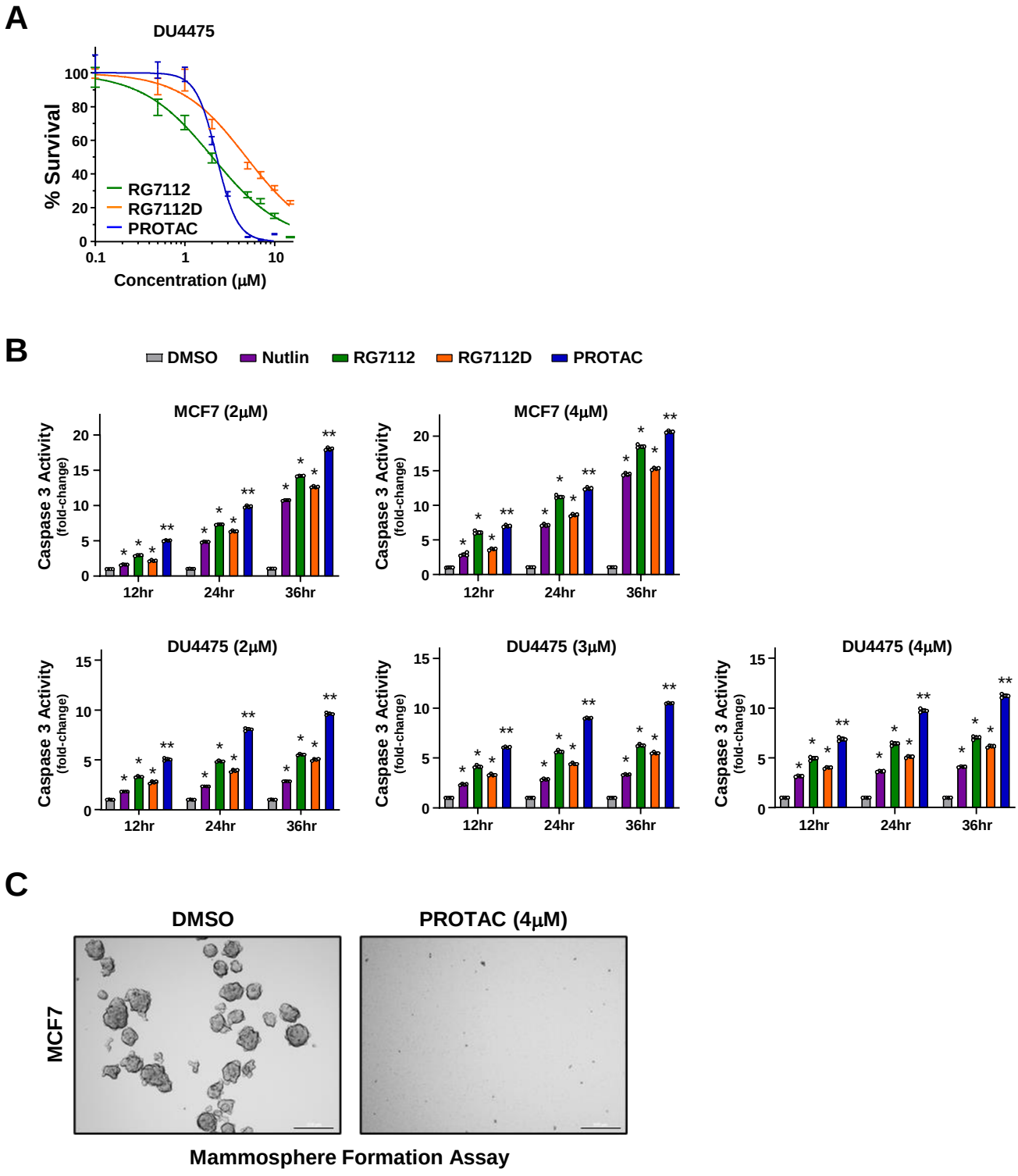
A
DU4475
% Survival
RG7112
RG7112D
PROTAC
Concentration (μM)
B
DMSO
Nutlin
RG7112
RG7112D
PROTAC
MCF7 (2μM)
MCF7 (4μM)
DU4475 (2μM)
DU4475 (3μM)
DU4475 (4μM)
Caspase 3 Activity
(fold-change)
12hr
24hr
36hr
C
DMSO
PROTAC (4μM)
MCF7
Mammosphere Formation Assay

Supplementary Figure S2. MDM2-PROTAC activates p53 and induces apoptosis of p53 wild-type breast cancer cell lines.

A, Following treatment of p53 wild-type DU4475 breast cancer cells with the indicated compounds or DMSO vehicle control, MTS survival assays (quadruplicate, 48hr) were performed. **B**, p53 wild-type MCF7 and DU4475 breast cancer cell lines were treated with the indicated compounds at the concentrations denoted and Caspase-3 activity (triplicate) was measured at intervals. **C**, Representative images of mammosphere formation of MCF7 cells in the presence of MDM2-PROTAC or DMSO control; scale bar is 300μm. Mean ± SD (**A**, **B**). For **B**, MCF7: **P*<0.00081, comparing each compound to DMSO vehicle control and ***P*<0.0025, comparing PROTAC to control compounds; DU4475: **P*<0.00021, comparing each compound to DMSO vehicle control and ***P*<0.0001, comparing PROTAC to control compounds; 2-way ANOVA.

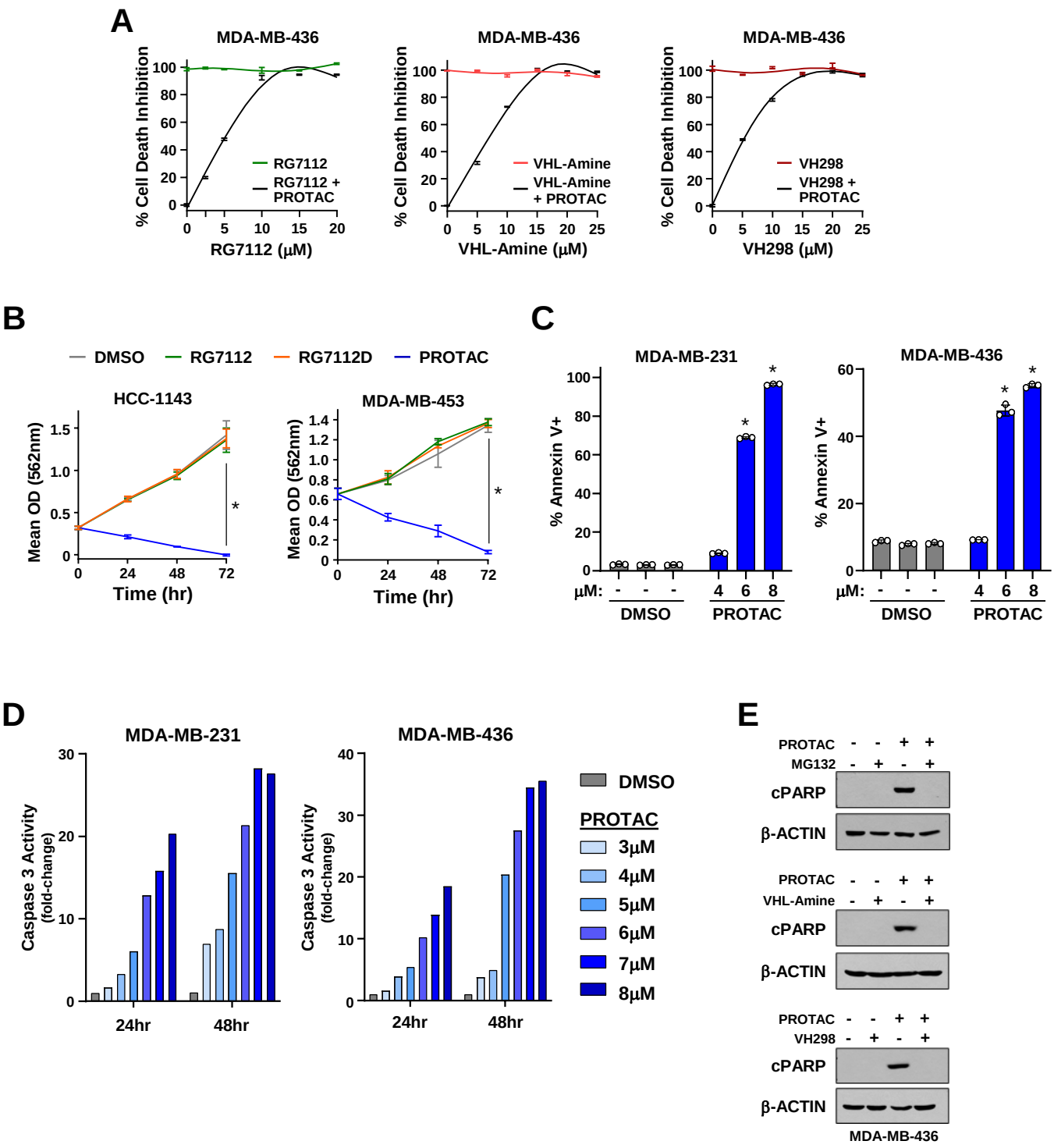
A
MDA-MB-436
% Cell Death Inhibition
RG7112
RG7112 + PROTAC
RG7112 (μM)
MDA-MB-436
VHL-Amine
VHL-Amine + PROTAC
VHL-Amine (μM)
MDA-MB-436
VH298
VH298 + PROTAC
VH298 (μM)
B
DMSO
RG7112
RG7112D
PROTAC
HCC-1143
MDA-MB-453
Mean OD (562nm)
Time (hr)
C
MDA-MB-231
MDA-MB-436
% Annexin V+
μM:
DMSO
PROTAC
D
MDA-MB-231
MDA-MB-436
Caspase 3 Activity (fold-change)
24hr
48hr
DMSO
PROTAC
3μM
4μM
5μM
6μM
7μM
8μM
E
PROTAC
MG132
cPARP
β-ACTIN
VHL-Amine
VH298
MDA-MB-436

Supplementary Figure S3. Apoptosis induced by MDM2-PROTAC treatment of p53-inactivated TNBC cells requires ternary complex formation and MDM2 proteosome-mediated degradation.

A, Inhibition of MDM2-PROTAC-induced death (quadruplicate, MTT survival assay, 48hr) in competition assays with the indicated compounds in MDA-MB-436 cells. **B**, MTT assays (quadruplicate) performed at 24hr intervals on HCC-1143 (p53-mutant) and MDA-MB-453 (p53-delete) TNBC cells treated with their IC_{50} (5μM and 6μM, respectively) of MDM2-PROTAC and equal concentrations of the control compounds or DMSO vehicle control. **C** and **D**, MDA-MB-231 and MDA-MB-436 cells were treated with increasing concentrations of MDM2-PROTAC or DMSO vehicle control (-) and apoptosis was measured by Annexin-V positivity (**C**, triplicate) and Caspase-3 activity (**D**). **E**, Western blots following treatment of MDA-MB-436 cells with the indicated compounds or DMSO (-). β-ACTIN blots are the same as in Fig. 1H, 1J, and 1K. Mean ± SD (**A-C**). For **B**, **P*<0.0017 (2-way ANOVA), comparing PROTAC to control compounds and DMSO vehicle control. For **C**, **P*<0.0001 (unpaired two-tailed *t*-tests), comparing PROTAC to DMSO vehicle control.

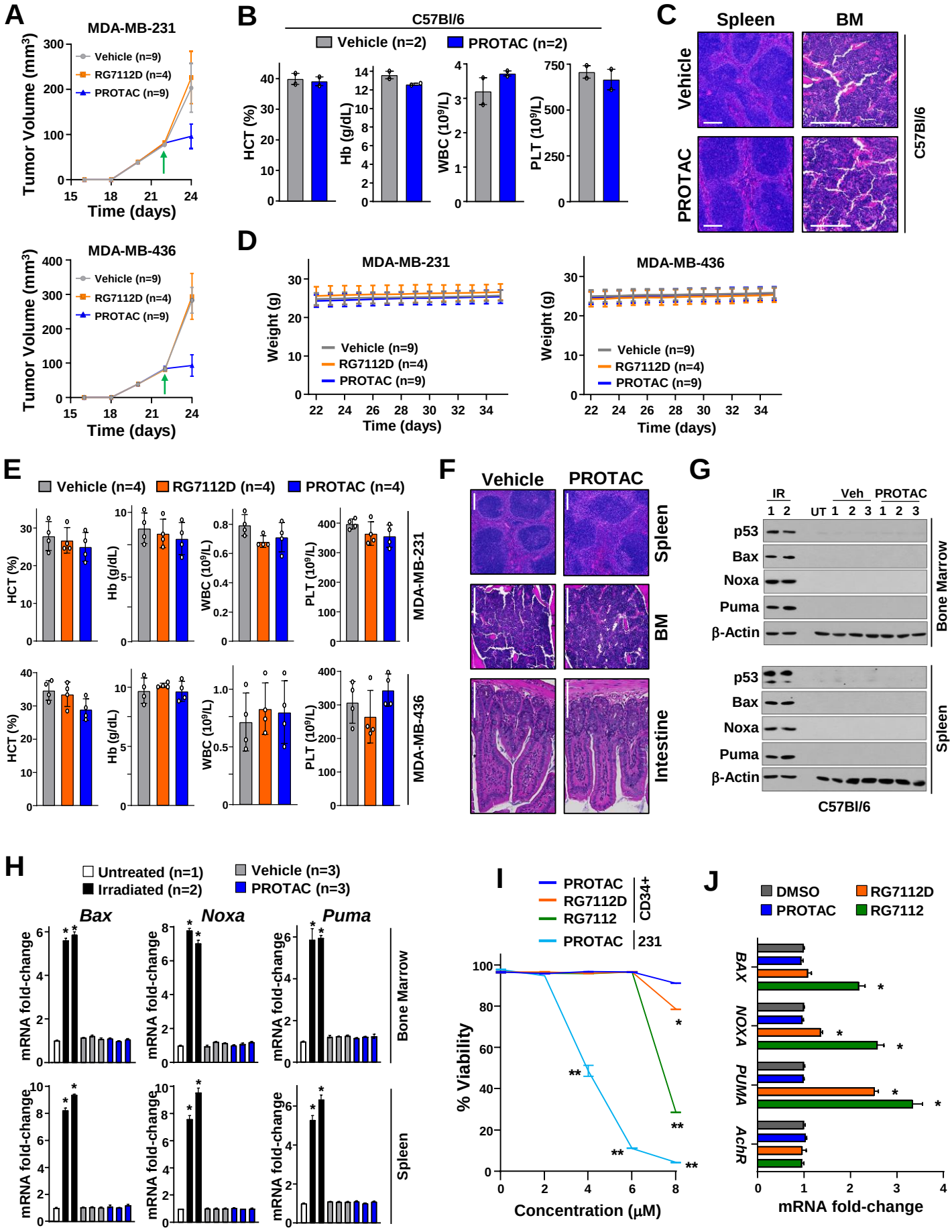
A
MDA-MB-231
Tumor Volume (mm³)
Vehicle (n=9)
RG7112D (n=4)
PROTAC (n=9)
Time (days)
MDA-MB-436
B
C57Bl/6
Vehicle (n=2)
PROTAC (n=2)
HCT (%)
Hb (g/dL)
WBC (10⁹/L)
PLT (10⁹/L)
C
Spleen
BM
Vehicle
PROTAC
C57Bl/6
D
MDA-MB-231
MDA-MB-436
Weight (g)
Time (days)
E
Vehicle (n=4)
RG7112D (n=4)
PROTAC (n=4)
MDA-MB-231
MDA-MB-436
F
Vehicle
PROTAC
Spleen
BM
Intestine
G
IR
UT
Veh
PROTAC
p53
Bax
Noxa
Puma
β-Actin
Bone Marrow
Spleen
C57Bl/6
H
Untreated (n=1)
Irradiated (n=2)
Vehicle (n=3)
PROTAC (n=3)
Bax
Noxa
Puma
mRNA fold-change
Bone Marrow
Spleen
I
PROTAC
RG7112D
RG7112
CD34+
PROTAC
231
% Viability
Concentration (μM)
J
DMSO
RG7112D
PROTAC
RG7112
BAX
NOXA
PUMA
AchR
mRNA fold-change

Supplementary Figure S4. No overt toxicities from the MDM2-PROTAC observed *in vivo*.

A, Tumor volumes of MDA-MB-231 and MDA-MB-436 subcutaneous xenografts in Fig. 5D prior to day 24, showing the size of palpable tumors (approximately 80mm^3) when treatment with MDM2-PROTAC, RG7112D, or vehicle control began (day 22, green arrow). **B** and **C**, After C57Bl/6 immunocompetent mice received intraperitoneal (IP) injections of MDM2-PROTAC (50mg/kg) or vehicle control twice daily for 8 consecutive days, complete blood counts were determined (**B**) and H&E sections of formalin-fixed paraffin-embedded tissues evaluated (**C**, BM-bone marrow). **D-F**, Nude mice with subcutaneous tumors of MDA-MB-231 and MDA-MB-436 TNBC cells were administered (IP) MDM2-PROTAC, RG7112D, or vehicle control (50mg/kg) for 14 consecutive days. Mouse weight was measured daily throughout the course of treatment (**D**), complete blood counts were determined following 13 consecutive treatments (**E**), and sections of formalin-fixed paraffin-embedded tissues from mice at time of sacrifice were H&E stained and evaluated (**F**). Representative images are shown and scale bars are 200μm (spleen) and 300μm (bone marrow and intestine). **G** and **H**, C57Bl/6 mice were treated (IP injection) with MDM2-PROTAC or vehicle control at 50mg/kg once daily for 3 consecutive days (n=3/group). After 72hr of treatment, mice were euthanized and whole bone marrow and splenocytes were harvested and protein and mRNA were evaluated by Western blotting (**G**) and qRT-PCR (**H**), respectively. Two gamma irradiated (IR) mice served as positive controls. **I** and **J**, Human CD34+ hematopoietic cells were treated with the compounds indicated or DMSO vehicle control at the indicated concentrations (**I**, 48hr) or 8μM (**J**, 24hr). Viability (**I**) was determined using a fluorescent live-dead flow cytometric assay, and mRNA levels were evaluated by qRT-PCR (**J**). Mean ± SD (**A**, **B**, **D**, **E**, and **H-J**). For H, $*P<9.61\text{x}10^{-5}$ for bone marrow and $*P<5.19\text{x}10^{-6}$ for spleen; for I, $*P=3.12\text{x}10^{-4}$ and $**P<1.51\text{x}10^{-3}$; and for J, $*P<9.57\text{x}10^{-5}$.

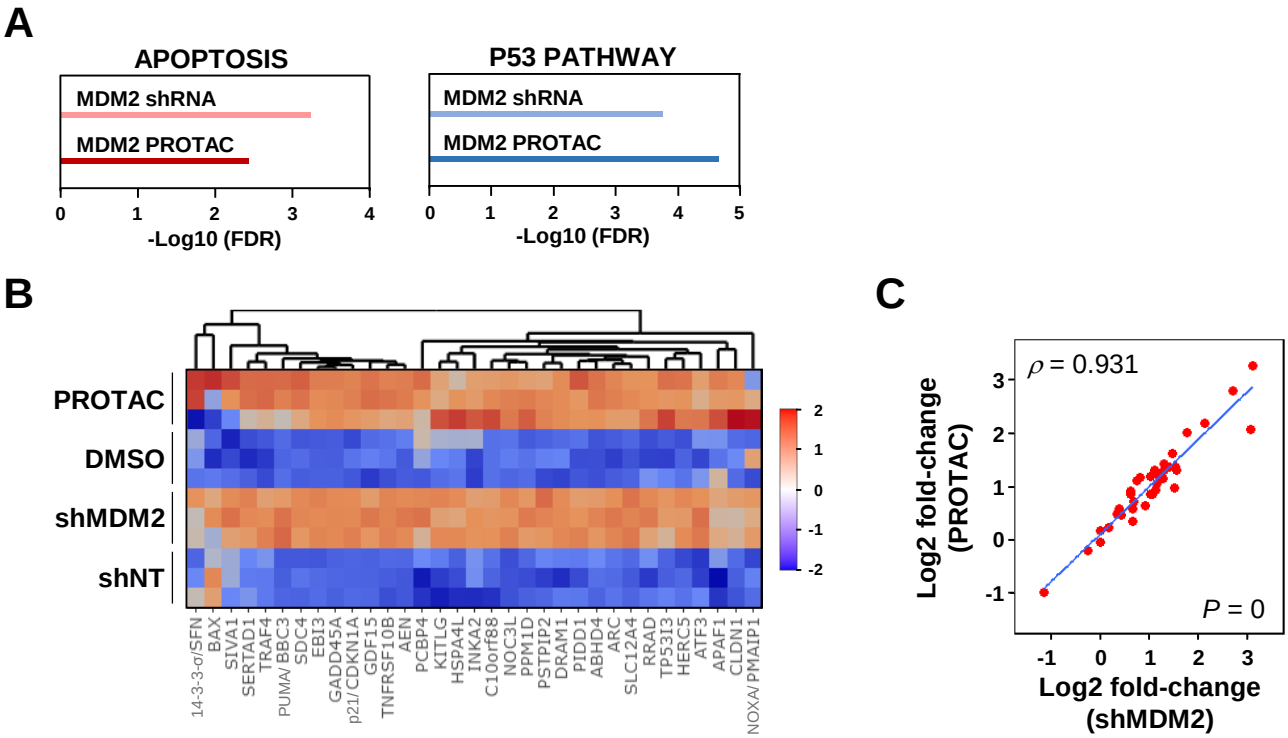
A
APOPTOSIS
MDM2 shRNA
MDM2 PROTAC
0 1 2 3 4
-Log10 (FDR)
P53 PATHWAY
MDM2 shRNA
MDM2 PROTAC
0 1 2 3 4 5
-Log10 (FDR)
B
PROTAC
DMSO
shMDM2
shNT
14-3-3-σ/SFN
BAX
SIVA1
SERTAD1
TRAF4
PUMA/ BBC3
SDC4
EBI3
GADD45A
p21/CDKN1A
GDF15
TNFRSF10B
AEN
PCBP4
KITLG
HSPA4L
INKA2
C10orf88
NOC3L
PPM1D
PSTPIP2
DRAM1
PIDD1
ABHD4
ARC
SLC12A4
RRAD
TP53I3
HERC5
ATF3
APAF1
CLDN1
NOXA/ PMAIP1
2 1 0 -1 -2
C
ρ = 0.931
P = 0
Log2 fold-change (PROTAC)
Log2 fold-change (shMDM2)
D
DMSO
PROTAC
mRNA fold-change
BAX NOXA PUMA AEN APAF1 TP53I3 PIDD1 AchR
shNT
shMDM2
mRNA fold-change
BAX NOXA PUMA AEN APAF1 TP53I3 PIDD1 AchR

Supplementary Figure S5. p53 family target genes are up-regulated following MDM2 degradation or *MDM2* knockdown in TNBC cells.

RNA-seq (triplicates) was performed on MDA-MB-436 cells treated with MDM2-PROTAC (6μM, 16hr) or DMSO vehicle control and cells expressing *MDM2* shRNA or non-targeting control shRNA (48hr). **A**, Pathway analysis using Hallmark gene signatures. **B**, Heatmap of p53 family target genes of individual samples (3 samples per group). **C**, Spearman's correlation of differential p53 family target gene expression between PROTAC-treated relative to DMSO vehicle control and *MDM2* shRNA relative to non-targeting shRNA control; Spearman's correlation coefficient (ρ) and P-value are indicated. **D**, qRT-PCR analysis (triplicate, 6μM, 16hr) to validate RNA-seq results; mean ± SEM. For **D**, **P*<0.0001 using unpaired two-tailed *t*-tests, comparing MDM2-PROTAC to DMSO vehicle control or *MDM2* shRNA to non-targeting control shRNA.

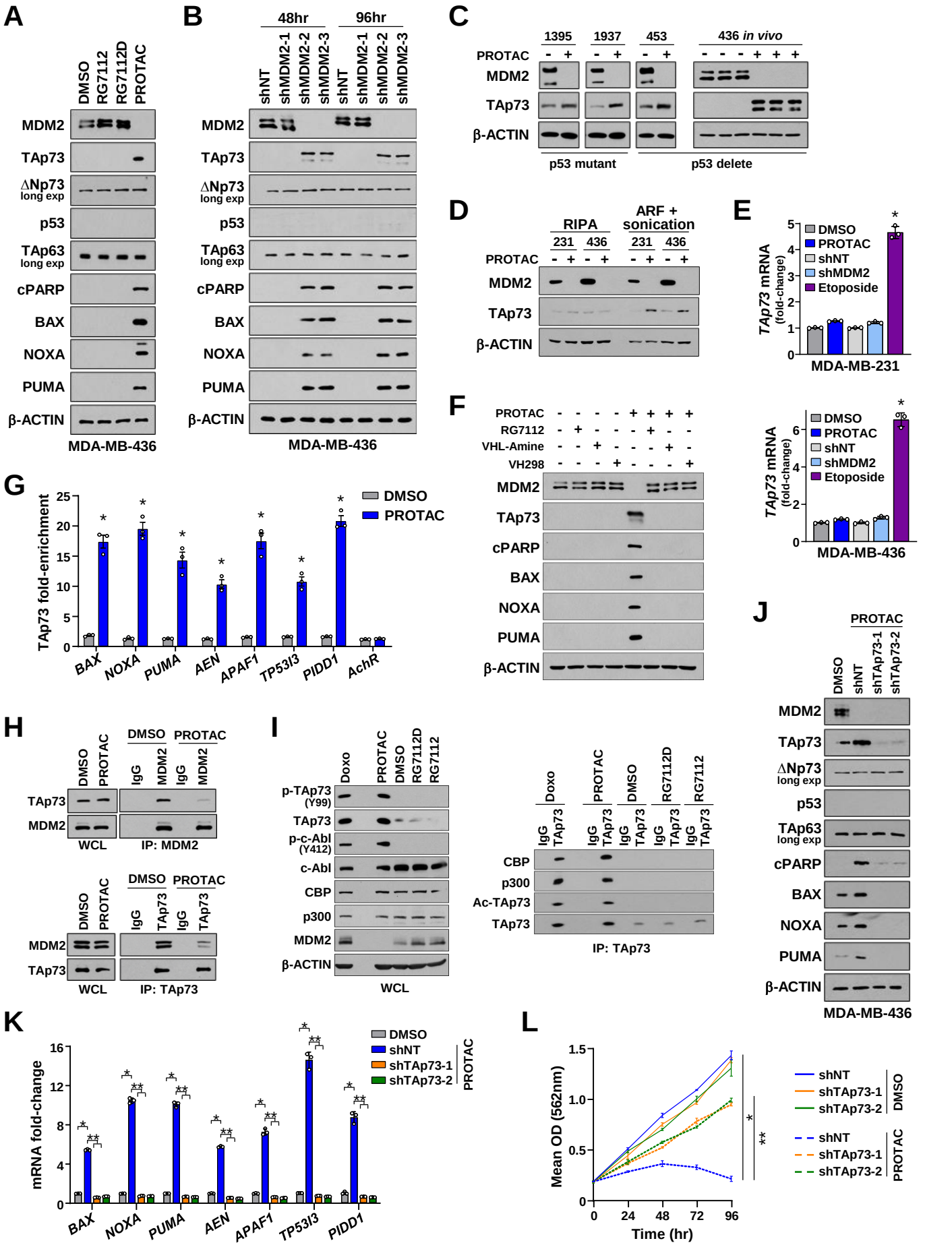
A
DMSO
RG7112
RG7112D
PROTAC
MDM2
TAp73
ΔNp73 long exp
p53
TAp63 long exp
cPARP
BAX
NOXA
PUMA
β-ACTIN
MDA-MB-436
B
48hr
96hr
shNT
shMDM2-1
shMDM2-2
shMDM2-3
MDM2
TAp73
ΔNp73 long exp
p53
TAp63 long exp
cPARP
BAX
NOXA
PUMA
β-ACTIN
MDA-MB-436
C
1395
1937
453
436 in vivo
PROTAC
MDM2
TAp73
β-ACTIN
p53 mutant
p53 delete
D
RIPA
ARF + sonication
231
436
PROTAC
MDM2
TAp73
β-ACTIN
E
TAp73 mRNA (fold-change)
DMSO
PROTAC
shNT
shMDM2
Etoposide
MDA-MB-231
F
PROTAC
RG7112
VHL-Amine
VH298
MDM2
TAp73
cPARP
BAX
NOXA
PUMA
β-ACTIN
TAp73 mRNA (fold-change)
DMSO
PROTAC
shNT
shMDM2
Etoposide
MDA-MB-436
G
TAp73 fold-enrichment
DMSO
PROTAC
BAX
NOXA
PUMA
AEN
APAF1
TP53I3
PIDD1
AchR
H
DMSO
PROTAC
IgG
MDM2
TAp73
WCL
IP: MDM2
IP: TAp73
I
Doxo
PROTAC
DMSO
RG7112D
RG7112
p-TAp73 (Y99)
TAp73
p-c-Abl (Y412)
c-Abl
CBP
p300
MDM2
β-ACTIN
WCL
IgG
TAp73
Ac-TAp73
IP: TAp73
J
PROTAC
DMSO
shNT
shTAp73-1
shTAp73-2
MDM2
TAp73
ΔNp73 long exp
p53
TAp63 long exp
cPARP
BAX
NOXA
PUMA
β-ACTIN
MDA-MB-436
K
mRNA fold-change
DMSO
shNT
shTAp73-1
shTAp73-2
PROTAC
BAX
NOXA
PUMA
AEN
APAF1
TP53I3
PIDD1
L
Mean OD (562nm)
Time (hr)
shNT
shTAp73-1
shTAp73-2
DMSO
PROTAC

Supplementary Figure S6. MDM2-PROTAC activates TAp73, which is then required to mediate apoptosis of p53-inactivated TNBC cells.

A-C, Western blotting was performed for the proteins indicated following treatment with MDM2-PROTAC, control compounds, or DMSO vehicle control (-) of MDA-MB-436 cells growing in culture (**A**, 6μM, 16hr), MDA-MB-436 subcutaneous tumors harvested 72hr after treatment began (**C**, right; MDM2 and β-ACTIN blots are same as in Fig. 5E), and in 3 additional TNBC cell lines (**C**, left), and following knockdown of *MDM2* with two shRNA or non-targeting shRNA (shNT) control (**B**). **D**, Western blots comparing lysis methods used to extract proteins. **E**, qRT-PCR (triplicate) for *TAp73* following treatment of MDA-MB-231 and MDA-MB-436 cells with MDM2-PROTAC (6μM, 16hr) or DMSO vehicle control or cells expressing *MDM2* shRNA or non-targeting control shRNA (48hr). Cells treated with etoposide (10μM, 24hr) were a positive control for *TAp73* expression. **F**, MDA-MB-436 cells pre-treated (1hr, 10μM) with RG7112, VHL-Amine, or VH298 were treated with MDM2-PROTAC (6μM, 16hr) or DMSO vehicle control (-) and the indicated proteins Western blotted. **G**, ChIP for TAp73 was performed with MDA-MB-436 cells following treatment with the PROTAC (6μM, 16hr) or DMSO vehicle control and enrichment of TAp73 (triplicate; first normalized to input DNA then IgG control) was determined at the loci indicated. **H**, MDA-MB-436 cells pre-treated with MG132 (1hr, 10μM) were treated with MDM2-PROTAC (6μM, 16hr) or DMSO vehicle control and MDM2 (top) and TAp73 (bottom) were immunoprecipitated and Western blots performed. **I**, MDA-MB-436 cells were treated with MDM2-PROTAC, RG7112D, RG7112 (all at 6μM, 16hr) or DMSO vehicle control. Proteins were Western blotted (left) and TAp73 was immunoprecipitated and then proteins Western blotted (right). **J** and **K**, MDA-MB-436 cells expressing two independent *TAp73* shRNA or non-targeting shRNA (shNT) control were treated with MDM2-PROTAC or DMSO vehicle control (6μM, 16hr). p53/TAp73 target genes were evaluated by Western blotting (**J**) and qRT-

PCR (**K**, triplicate). **L**, MTT assay (quadruplicate, every 24hr) of MDA-MB-436 cells with two independent *TAp73* shRNA or non-targeting shRNA (shNT) control treated with MDM2-PROTAC or DMSO vehicle control (4μM). Mean ± SEM (**E**, **G**, **K**) and mean ± SD (**L**). For **E**, **P*<0.0001 (1-way ANOVA), comparing MDM2-PROTAC or etoposide to DMSO vehicle control or *MDM2* shRNA to non-targeting control shRNA. For **G**, **P*<0.0001 (unpaired two-tailed *t*-tests), comparing PROTAC to DMSO vehicle control. For **K**, **P*<0.0034, comparing non-targeting control shRNA with PROTAC to DMSO vehicle control and ***P*<0.0039, comparing *TAp73* shRNA with PROTAC to non-targeting shRNA control with PROTAC; 2-way ANOVA. For **L**, **P*<0.0001, comparing non-targeting control shRNA with PROTAC to DMSO vehicle control and ***P*<0.0099, comparing *TAp73* shRNA with PROTAC to non-targeting shRNA control with PROTAC; 2-way ANOVA. For A, B, and J, long exp is long exposure.

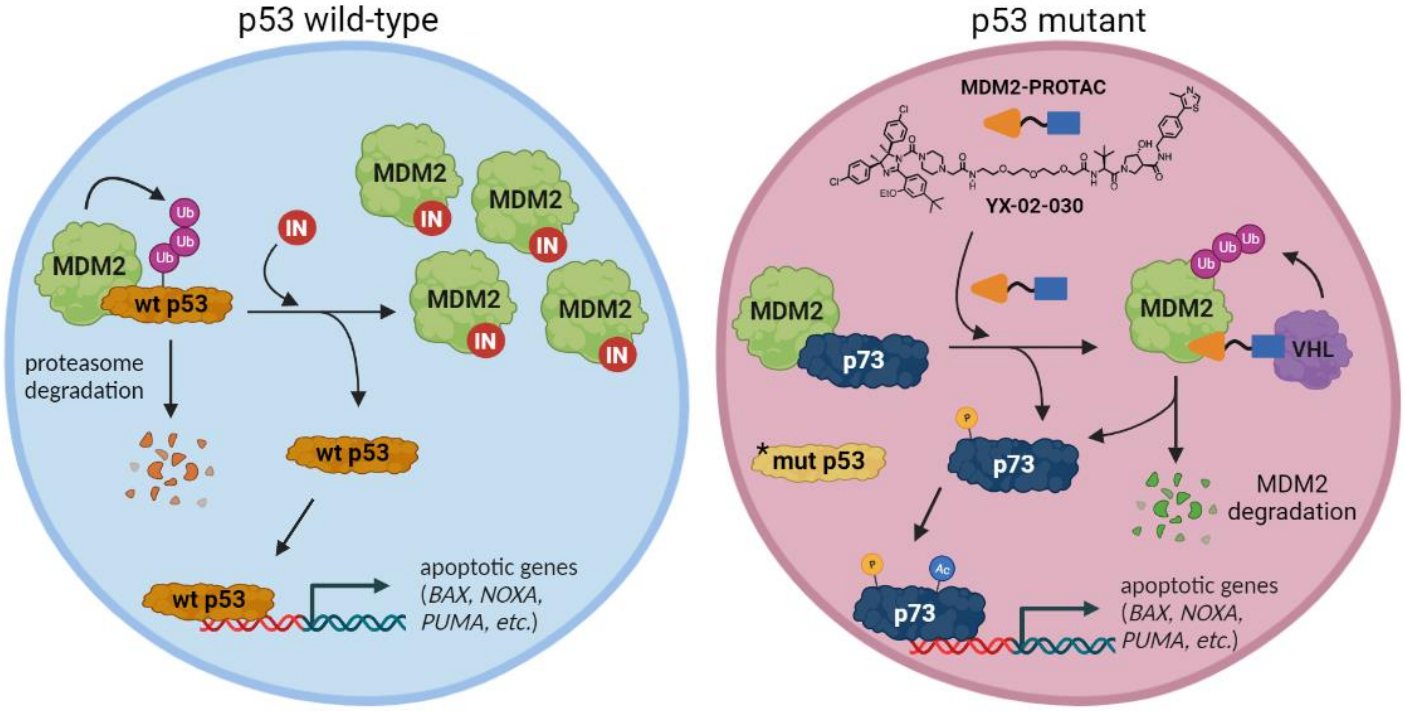
p53 wild-type
MDM2
Ub
Ub
Ub
wt p53
IN
MDM2
IN
MDM2
IN
MDM2
IN
MDM2
IN
proteasome
degradation
wt p53
wt p53
apoptotic genes
(BAX, NOXA,
PUMA, etc.)
p53 mutant
MDM2-PROTAC
YX-02-030
MDM2
p73
MDM2
Ub
Ub
VHL
*mut p53
P
p73
MDM2
degradation
P
Ac
p73
apoptotic genes
(BAX, NOXA,
PUMA, etc.)

Supplementary Figure S7. Graphical summary of the conclusions of the study.

MDM2 inhibitors are designed to disrupt MDM2:p53 binding, thereby preventing negative regulation of wild-type p53 by MDM2, which allows p53 to function as a tumor suppressive transcription factor. MDM2 inhibitors are only effective in cancer cells with wild-type p53, but they result in a toxic build-up of MDM2 in the cell. We designed and synthesized an MDM2-PROTAC that effectively targets MDM2 for degradation, leading to TAp73 phosphorylation and acetylation, which results in its stabilization and transcriptional activation. This allows TAp73 to orchestrate an apoptotic program in place of p53 in p53 mutant (and deleted) TNBC cells. Our MDM2-PROTAC reveals a new potential therapeutic target for treating aggressive and therapy-resistant p53-inactivated TNBC. This figure was created with BioRender.com and was exported under an academic subscription.